Tracking Lung Tumor Regression During Radiotherapy Using 5DCT-Driven Motion-Compensated CBCT

R. Andosca, P. Boyle, C. Miller, M. Lauria, D. Moghanaki, J. Neylon, D. O'Connell, D. Low

Department of Radiation Oncology, UCLA, Los Angeles, CA

2026 JULY 19–22 VANCOUVER, BC
JOINT AAPM | COMP MEETING

ABSTRACT

Standard cone-beam CT (CBCT) poorly tracks lung-tumor response because breathing motion blurs tumor edges. We applied motion-compensated SART (mcSART) — which deblurs each daily CBCT using a patient-specific 5DCT-derived deformation model driven by a bellows breathing surrogate — across a full 30-fraction lung course.

Daily mcSART enabled reliable coronal tumor measurement: a 19.5% regression (69.6 → 56.0 mm) that agreed across three motion models and with 5DCT references. A fully automated, observer-free voxel analysis independently reproduced the same downward trend — supporting routine CBCT as a no-added-dose tool for quantitative response monitoring.

KEY FINDINGS

19.5%
Coronal tumor-diameter reduction (69.6 → 56.0 mm)

≈1.5 mm
Mean agreement across the 3 motion models

≤0.3 mm
Deviation from 5DCT references (fx 1 / 12 / 22)

2.9%
Automated inter-model spread (of a ~20% signal)

0
Added dose or extra appointments

CONTACT

Ryan Andosca
Dept. of Radiation Oncology, UCLA
randosca@mednet.ucla.edu

Scan to email

INTRODUCTION

Most lung-cancer patients finish radiotherapy with no quantitative measure of tumor response. Diagnostic CT adds dose and appointments, while the CBCT taken before each fraction is degraded by respiratory-motion artifacts that blur tumor boundaries in the thorax.

Regression can go undetected until post-treatment imaging — missing chances for adaptive replanning. mcSART recovers motion-deblurred tumor edges from projections already acquired daily, turning routine CBCT into a response-monitoring tool with no extra dose or appointments.

METHODS & MATERIALS

Patient & data
One lung-cancer patient (tumor abutting the mediastinum); 30 fractions over ~6 weeks.

mcSART
Each daily CBCT (~900 projections) is reconstructed by warping the volume to the breathing state of every projection — from a simultaneous bellows surrogate — then forward-projecting, comparing, and back-projecting, with GPU-accelerated DVF inversion. No phase binning: each projection gets its own state-specific correction.

Synchronization
Bellows and gantry clocks are aligned by a video-based calibration plus a diaphragm temporal calibration.

Models & measurement
Three 5DCT-derived motion models (planning + rescans at fx 12 & 22) were applied to most fractions (90 mcSART volumes). The coronal longest diameter (RECIST 1.1; superior–inferior axis, most affected by breathing) was measured per fraction in MIM, with 5DCT references at fx 1, 12, 22.

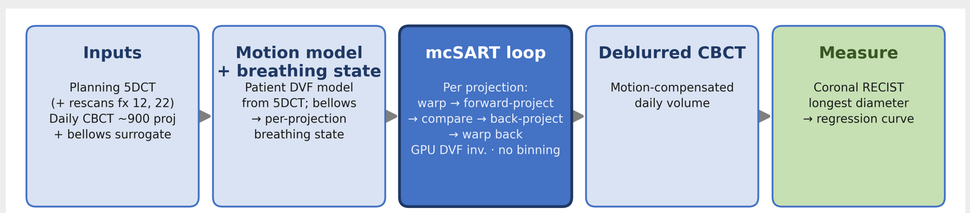

mcSART reconstruction and tumor-measurement workflow.

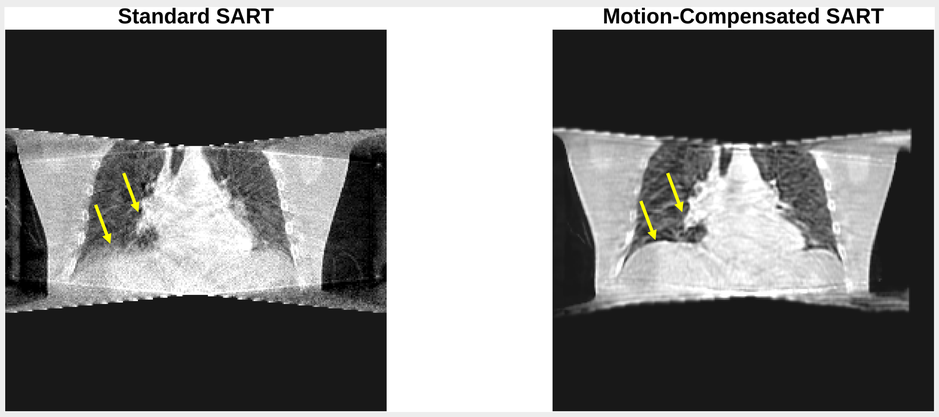

Fig. 1. Coronal CBCT, fraction 1: standard SART (left) vs motion-compensated SART (right). mcSART sharpens diaphragm, lung, and tumor margins blurred by motion. Arrows point to example areas where the image-quality increase is apparent. The window and level are identical for the two images.

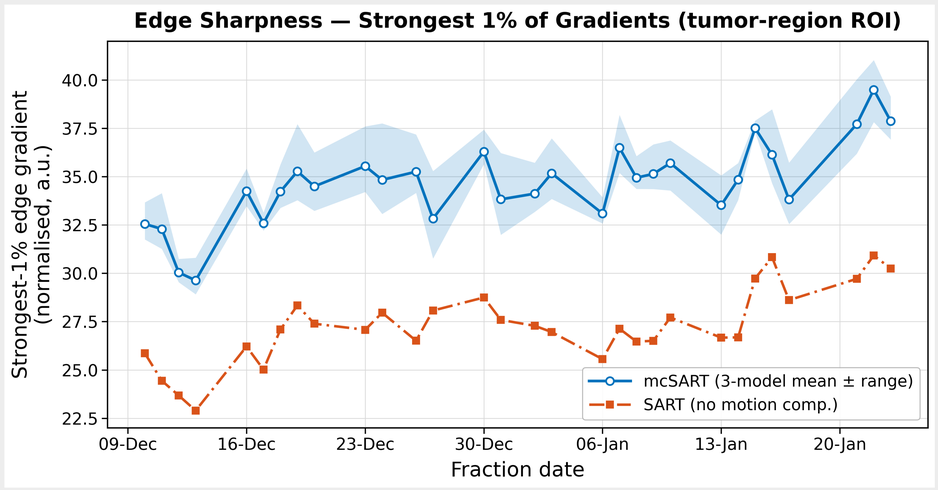

Fig. 2. Edge sharpness (mean of the strongest 1% of intensity gradients, contrast-normalized) in the tumor-region ROI. mcSART exceeds SART at every fraction — ~27% higher (median), with no overlap (band = range across the 3 motion models) — quantifying the motion-blur reduction seen at left. No tumor contour is used; the ROI also contains nearby vessels and the mediastinal interface (edge sharpness in the tumor region, not of the tumor boundary). Because both reconstructions share the same fractions, regression cancels and the gap reflects the deblurring, not the response.

RESULTS

mcSART recovered diaphragm, lung, and tumor edges that standard SART smears (Fig. 1). Edge sharpness in the tumor region was ~27% higher for mcSART than SART at every fraction (Fig. 2). The coronal longest diameter fell 69.6 → 56.0 mm — a 19.5% reduction over 30 fractions (Fig. 3; ±0.75 mm precision). The three motion models agreed within ~1.5 mm on average and deviated from 5DCT references by only 0.2 / 0.3 / 0.2 mm at fractions 1 / 12 / 22. A fully automated, observer-free voxel analysis independently reproduced the trend (Fig. 4): the tumor attenuation — a surrogate for tumor size — fell to ~76% of baseline, with the three reconstructions agreeing to a mean of 2.9 pp per fraction against a ~20% regression signal.

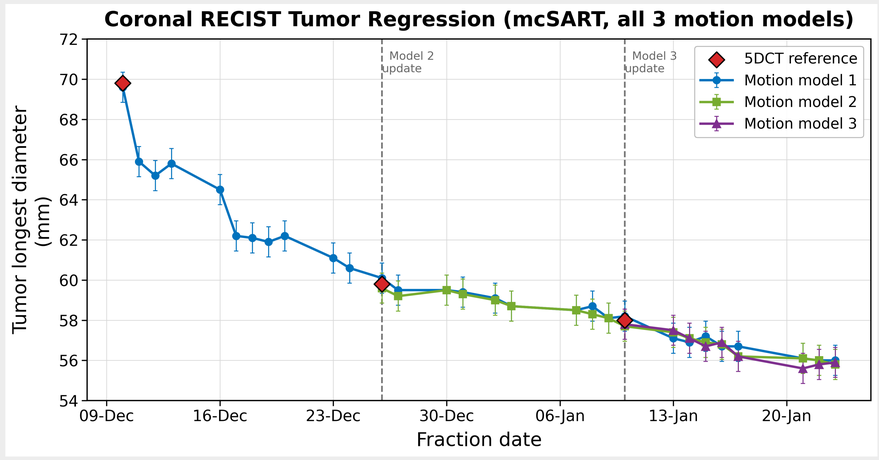

Fig. 3. Primary result — coronal RECIST longest diameter per fraction (3 motion models). 69.6→56.0 mm (19.5%); error bars ±0.75 mm; red diamonds = 5DCT references; dashed lines = model updates; fraction 18 unavailable due to reconstruction issues which were resolved after this measurement was acquired.

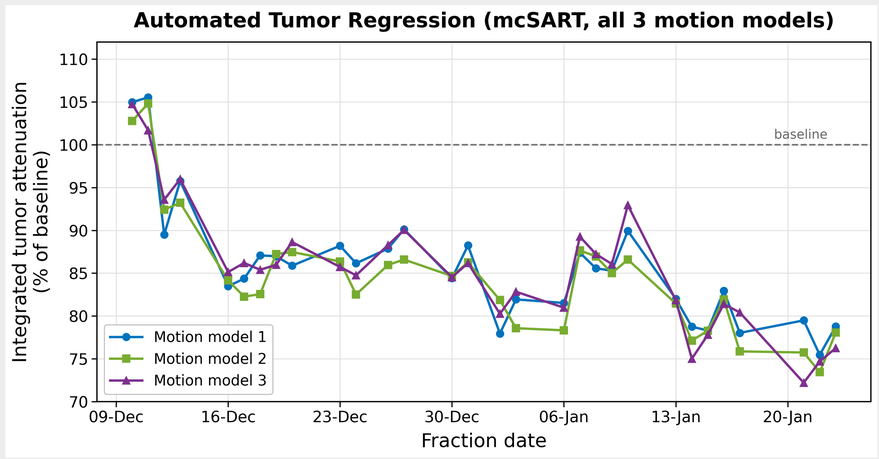

Fig. 4. Independent corroboration — automated, observer-free integrated tumor attenuation (a surrogate for tumor size), all 3 motion models; falls to ~76% of baseline. Three reconstructions track closely (mean spread 2.9 pp). Absolute magnitude is an upper bound (see Discussion); the trajectory is robust.

DISCUSSION

Two independent measurements — expert coronal RECIST and a fully automated voxel analysis — agree the tumor regressed ~20% over the course, showing motion-deblurred daily CBCT can quantify response from data already acquired.

Agreement across three motion models, and the close match to periodic 5DCT references, indicate the patient-specific model stays valid over multi-week treatment and that mid-treatment rescans may be unnecessary.

Caveat: the automated magnitude is an upper bound: a static-shell QC residual rises late in treatment, so registration/intensity drift pads the absolute change; the trajectory is robust, the magnitude approximate. Baseline subtraction removes each model's offset, so inter-model agreement reflects a model-robust trajectory, not pixel-identical reconstructions.

CONCLUSIONS

mcSART enables quantitative daily lung-tumor tracking that standard CBCT cannot using only routine projections and an external surrogate, with no added dose or appointments. A clear 19.5% regression was tracked with millimeter precision and corroborated by a fully automated analysis, supporting mcSART-derived CBCT as an adaptive-replanning trigger.

Future work: multi-patient validation, multi-observer and volumetric measurement, registration refinement, and dose-accumulation studies.

REFERENCES

1. Lauria M, et al. Motion compensated cone-beam CT reconstruction using an a priori motion model from CT simulation. Phys Med Biol 2024;69(7):075022.
2. Low DA, et al. Novel breathing motion model for radiotherapy. Int J Radiat Oncol Biol Phys 2005;63(3):921–929.
3. Low DA, et al. A method for the reconstruction of four-dimensional synchronized CT scans during free breathing. Med Phys 2003;30(6):1254–1263.
4. Chen M, et al. A simple fixed-point approach to invert a deformation field. Med Phys 2008;35(1):81–88.
5. Eisenhauer EA, et al. New response evaluation criteria in solid tumours: RECIST v1.1. Eur J Cancer 2009;45(2):228–247.
6. Jaffray DA, et al. Flat-panel cone-beam CT for image-guided radiation therapy. Int J Radiat Oncol Biol Phys 2002;53(5):1337–1349.
7. Sonke JJ, Belderbos J. Adaptive radiotherapy for lung cancer. Semin Radiat Oncol 2010;20(2):94–106.